JCTC Journal of Chemical Theory and Computation

Article

pubs.acs.org/JCTC

Free-Energy Landscape of a Thrombin-Binding DNA Aptamer in Aqueous Environment

Eunae Kim,[†,‡] Changwon Yang,[§] and Youngshang Pak[§,*]

[†]*BK-21* Project Team, College of Pharmacy, Chosun University, Gwangju 501-759, Republic of Korea

[‡]Supercomputing Center, Korea Institute of Science and Technology Information, Daejeon 305-806, Republic of Korea

[§]Department of Chemistry and Institute of Functional Materials, Pusan National University, Busan 609-735, Republic of Korea

ABSTRACT: Thrombin-binding aptamer (TBA-15) is a single-stranded 15-mer oligonucleotide that has a wide range of biomedical applications. In the presence of metal cations of proper sizes, this aptamer displays G-quadruplexes with a single cation enclosed at its central binding site when it is completely folded. To understand how this aptamer folds into its stable three-dimensional structure in the presence of K^+ ions, we carried out free-energy calculations using the state-of-art replica exchange molecular dynamics simulation (REMD) at the all-atom level. The resulting free energy map revealed that TBA-15 follows a two-state folding behavior with a substantially large folding barrier of 6 kcal/mol at ambient temperature. Our simulation showed that the intervening TGT-loop, which is located in the middle of the TBA-15 sequence, virtually remains intact regardless of folding and unfolding states. Furthermore, in the conserved TGT-loop structure, the base-pair stacking of G8 and T9 induces the native-like base orientations of G6 and G10 pertaining to the upper G-quadrant. This stacking interaction enhances the loop stability and reduces its dynamic fluctuations. Interestingly, for the G-stem to fold into its native state, the aggregation of the G8 and T9 residues in the TGT-loop is a key step for initiating the folding event of the G-stem by capturing a bulky cation.

INTRODUCTION

In drug design, DNA aptamers are attractive candidates for various diseases because of their highly specific binding affinity with various ligands.[1−5] Among numerous aptamers, the thrombin binding aptamer (TBA-15) is a widely investigated single-stranded DNA segment. TBA-15 is a 15-mer oligonucleotide with a sequence of 5′-GGTTGGTGTGGTTGG-3′. This is the simplest possible DNA sequence leading to two consecutive G-quadruplexes stacked in antiparallel fashion (Figure 1). As shown by NMR[6,7] and X-ray[8] experiments, TBA-15 forms two planar G-quartets along with two TT-loops and one TGT-loop. In particular, the TT-loops play a role in specific binding with the serine protease thrombin during the blood coagulation process.[9] The TGT-loop in the middle of the aptamer sequence interacts with the upper quadruplex plane of the native state (G1-G6-G10-G15 residues) and increases the stability of the G-quadruplexes.[10] This antiparallel stacking of two neighboring quartets creates a central binding site that can accommodate a single metal cation of K^+, NH_4^+, or Sr^{2+}.[11] Usually, this cation is coordinated with eight carbonyl oxygen atoms (atom type O6) of the two quartets, and the four coplanar guanines of the G-quartets are stabilized by the Hoogsteen hydrogen bonding.[12] The cation binding to the G-stem appears to be a key factor in governing the stability of the G-quadrants in aqueous environments. Several thermodynamic experiments on the aptamer/cation complex have been performed to obtain detailed thermodynamic parameters on TBA-15 folding in the presence of metal cations.[13−18] Also, all-atom level molecular dynamics (MD) simulations on TBA-15 were carried out to further reduce the gap between the theoretical and experimental outcomes.[19−24] Although recent MD simulations have substantially increased our understanding of the structure and dynamics of TBA-15 in the presence of cations, free-energy-based interpretations of overall folding mechanisms and the role of cations during the formation of the TBA-15/cation complex have not been available. In particular, free-energy simulations of the aptamer/K^+ complex can give more insight into its folding in atomic detail. Previously, using an umbrella sampling MD, we attempted to investigate the unfolding potential of mean force (PMF) of this aptamer upon

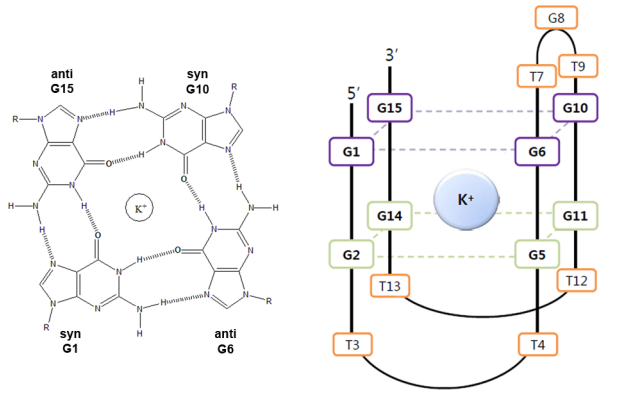

Figure 1. Schematic structure of thrombin binding aptamer TBA-15/K^+ complex and the base orientation of the coplanar G-quadruplex. The intramolecular G-quadruplexes consist of two parallel G-quadrant planes, two laterally bridged TT-loops, and one TGT-loop at the center of the aptamer sequences. The upper G-quadrant plane (G1, G6, G10, and G15) is colored purple, and the lower one (G2, G5, G11, and G14) is colored green. All three loops are represented by orange.

Received: August 14, 2012
Published: October 8, 2012

 © 2012 American Chemical Society

forced-stretching in the presence of a metal cation (Sr^{2+}).[24] However, the PMF cannot be directly transferred to the free-energy-based interpretation of the aptamer folding event due to the artifact of the one-dimensional (1D) pulling coordinate.

Therefore, in this work, we mapped the free-energy landscape of TBA-15/K^+ complex formation in K^+-rich aqueous conditions using the all-atom replica exchange molecular dynamics simulation (REMD) method. In our simulation study, the free-energy map of the aptamer/K^+ complex exhibits two-state folding behavior with a large folding barrier (6 kcal/mol). Consistent with the experimental values,[14] the folded state is only marginally stable compared to the unfolded state (ΔG = 1.2 kcal/mol). According to the free-energy profiles with various reaction coordinates at 288 K, the hairpin shape of the TGT-loop is maintained in either the folded or unfolded state. In particular, the base stacking of G8 and T9 in the TGT-loop appears to be a preliminary step for guiding the G-quadrant formation. As a bulky cation approaches the G-stem bases, the eight guanines of the G-stem capture the cation simultaneously to form the G-quadruplex assembly.

METHOD

Molecular Modeling. The NMR native structure of TBA-15 was determined at 288 K and taken from the protein data bank (PDB entry 1C34).[7] From the NMR native structure of TBA-15, the TBA-15/K^+ complex structure was also derived (PDB entry 1C35). In this case, the K^+ position in the G-DNA was obtained by a molecular modeling under a simple dielectric medium with the DNA part fixed. In this modeling, however, fixing DNA positions could lead to a potential bias in the predicted K^+ position, since this constraint prevents key gating motions of the guanine bases for possible ion movements. In the current work, following the procedure of Reshetnikov et al.,[23] a single K^+ ion was placed in the center of the G-quadruplexes. This DNA/K^+ complex structure was then solvated with a total of 3194 TIP3P water[25] molecules in a cubic simulation box with a size of 55.4 Å. Including the K^+ ion inserted into the central binding site, a total of 14 K^+ ions were added to the system to simulate a K^+-rich aqueous environment and to neutralize the total charge. The param99bsc0 force field was employed for the DNA segment.[26] For potassium ion, the standard AMBER parameters were used (σ = 0.2658 Å and ε = 0.000328 kcal/mol).[27] The whole system was subject to 50 ns MD run for thermal equilibration at 288 K (the NMR temperature). During the equilibration process, the G-quadrants with the potassium ion in its central binding region were well preserved, but the TT-loops displayed some distortion from the NMR position.

Molecular Dynamic Simulation and Analysis. As an enhanced conformational search for the free-energy mapping, the replica exchange molecular dynamics (REMD) simulation was used.[28] For the REMD simulation, a total of 58 replicas were employed to cover a temperature range of 271−485 K using the modified Berendsen thermostat.[29] Starting from the native structure of TBA-15/K^+ complex in the explicit water solvent, the initial conformation of each replica was prepared by running a normal MD for 50 ns at each replica temperature. All simulations were carried out with a time step of 2 fs using the LINCS algorithm[30] to fix the molecular bonds containing hydrogen and heavy atoms. The electrostatic interactions were calculated by the particle mesh Ewald method[31,32] with a cutoff distance of 10 Å. An exchange interval of 1 ps was employed and the trajectory was saved every 1 ps. The REMD simulation was performed with the GROMACS program.[33] In the present simulation, each replica was run for 350 ns, so that the total simulation time was 20.3 μs. After a full convergence toward equilibrium was achieved, using a proper set of two-dimensional (2D) reaction coordinates, the free energy surface was computed by $\Delta G = -RT \ln P(x,y)$, where $P(x,y)$ is the probability distribution function at the reaction coordinates of x and y. R and T are the gas constant and the absolute temperature, respectively.

RESULTS AND DISCUSSION

Figure 1 illustrates the TBA-15 structure in complex with a single K^+ ion. The K^+ ion is trapped in the central binding site consisting of the purine bases of the two parallel G-quadruplexes. The eight-guanine base stacking of the G-stem is alternatively in *anti*−*syn*−*anti*−*syn* glycosidic conformation. Each guanine makes four hydrogen bonds with two neighbor guanines.

Sampling and Convergence of the REMD. To monitor the sampling efficiency and reasonable convergence of the REMD simulation, several profiles were generated (Figure 2). Figure 2a shows the exchange traces of given replicas at temperatures of 288 K, 350 K, and 485 K. The exchange history of the three different replicas shows that the REMD simulation

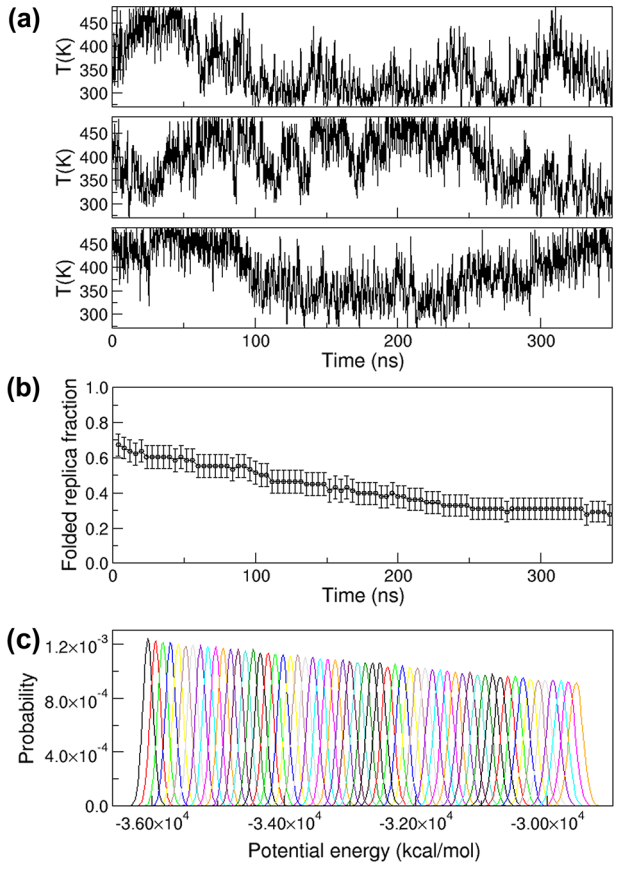

Figure 2. (a) Replica exchange history of replica exchange molecular dynamics (REMD) simulation. Here, the tracing results of three different replicas at 288, 350, and 485 K are given. (b) Profile of the folded replica fraction with time. After the initial 200 ns, the folded replica fraction reaches a steady-state value. (c) The potential energy distributions of all 58 replicas covering the temperature range 271−485 K.

explores a broad temperature space. In Figure 2b, the fraction of the folded replicas is given with respect to the simulation time. The folded replica was defined when a backbone root-mean-square deviation (rmsd) ≤ 4.0 Å. Since the simulation started from the folded conformation, most replicas at the beginning of the simulation have a backbone rmsd value of less than 4.0 Å in comparison with the NMR structures (PDB entry 1C34). After 200 ns, the folded replica number appears to reach a steady-state value. Thus, the simulation data from the initial 200 ns were excluded for the free-energy mapping. The potential energy distributions of all 58 replicas, which were also obtained after discarding the initial 200 ns, were shown in Figure 2c. For the present REMD simulation, the acceptance ratio of the exchange attempt was about 35%.

TBA-15 Folding Free-Energy Landscapes. To describe the overall TBA-15 folding, two-dimensional (2D) free-energy maps at four different temperatures (288, 306, 350, and 485 K) were constructed using two reaction coordinates: (1) the coordination number (CN) between K^+ and the eight O6 atoms of the G-quadrants and (2) the radius of gyration (R_g) of the eight guanine bases of the G-stem (Figure 3). As shown in Figure 3, with respect to temperature changes, the location of transition state (TS) remains intact and only the relative populations of the folded and unfolded states vary, indicating a typical two-state folding behavior. Also, consistent with the earlier MD simulation result,[23] the present result confirmed that the formation of a 1:2 complex between TBA-15 and K^+ is a remote possibility. In fact, a 1:2 complex in which the coordination number between O6 and K^+ exceeds eight appears to exist at elevated temperatures of 306 and 350 K (Figures 3b, c), but its population is virtually negligible. At the experimental temperature of 288 K (Figure 3a), the free-energy difference between the folding and the unfolding states is 1.2 kcal/mol, which agrees with the experimental values of 1.1−2.0 kcal/mol.[14] Moreover, the lowest free-energy minimum structure located at (CN, R_g) = (8.0, 5.0 Å) has a backbone rmsd of 3.0 Å, which is comparable to the NMR native structure.

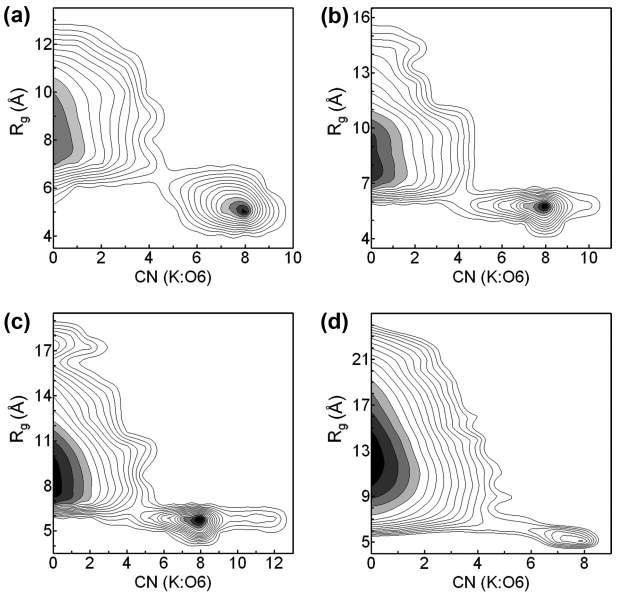

Figure 3. Two-dimensional (2D) free-energy surface at various temperatures: (a) 288 K, (b) 306 K, (c) 350 K, and (d) 485 K. The *X*-axis is the coordination number (CN) of K^+ with eight carboxylic oxygen atoms (atom type O6) of the G-stem (G1, G2, G5, G6, G10, G11, G14, and G15). The *Y*-axis is the radius of gyration (R_g) of eight purine bases in the G-stem. The folding pattern of the TBA-15/K^+ complex indicates a two-state folding mechanism. The line interval is about 0.5 kcal/mol in the map.

A previous MD simulation study dealt with prefolded G-quadrants subsequently enclosing a bulky cation at constant temperature.[21] In this case, the TGT-loop not only acted as a gate for capturing and releasing the cation but also increased the stability of the G-quadrants/K^+ complex by closing the gate. One remaining issue with this interpretation is the stability of the G-quadrants without the cation binding. On the free-energy map in Figure 3a, the conformation of the cation-free G-quadrants is located at (CN, R_g) = (0.0, 5.0 Å) at 288 K. Surprisingly, the free energy value of the cation-free G-tetrads is higher than that of the cation-bound G-quadrants by 7 kcal/mol. Therefore, in a realistic folding scenario at ambient temperature, it is unlikely that the TBA-15 folding occurs in such a way that the folding from the cation-free G-quadrants is immediately followed by binding with K^+. Thus, a more general picture of the TBA-15 folding in the context of overall folding/unfolding events is still needed.

Role of the TGT-Loop. A recent MD simulation indicated that the TGT-loop plays a key role in the metal binding and stability of the G-stem.[21] In this work, the role of the TGT-loop is re-examined based on the interpretation of free-energy landscapes of the aptamer/cation complex. Figure 4a shows the free-energy map at 288 K with respect to the backbone rmsd of the TGT-loop and the CN of K^+ with the O6 atoms of eight guanine bases in the G-stem. Notably, the rmsd value of the TGT-loop was not much different between the unfolded (rmsd = 2.5 Å) and the folded basin (rmsd = 2.0 Å), demonstrating that the hairpin shape of the TGT-loop is reasonably well maintained, even in the unfolded state of the G-stem. One difference in this loop between the folded and unfolded states is the more pronounced loop fluctuation in the unfolded state. Noting that the TGT-loop (T7-G8-T9) is located at the center

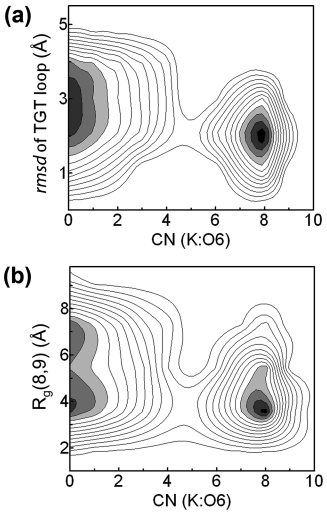

Figure 4. 2D free-energy landscapes (a) with the backbone rmsd of TGT-loop from the NMR native structure and the coordination number of K^+ with the O6 atoms in the G-stem [CN (K:O6)] and (b) with the radius of gyration of the purine (G8) and pyrimidine (T9) bases and CN (K:O6) at 288 K. For calculation of the backbone rmsd, the backbone atoms include P−O5′−C5′−C4′−C3′−O3′. The line interval is about 0.5 kcal/mol in the map.

dx.doi.org/10.1021/ct300714u | J. Chem. Theory Comput. 2012, 8, 4845−4851

of the TBA-15 sequence, this prefolded TGT-loop structure can effectively reduce the entropic cost for exploring the conformational space for the G-stem residues.

After thoroughly investigating the TGT-loop conformations, we found that the aggregation of G8 and T9 seems to be of a particular importance as a valuable descriptor of the folding event. To represent the aggregation state of this base-pair in the free-energy mapping, we introduced the radius of gyration [R_g(8,9)] of the purine base of G8 and the pyrimidine base of T9. Figure 4b shows the corresponding 2D free-energy profile with respect to the R_g(8,9) value and the CN between K^+ and O6 atoms of the G-stem. As shown in Figure 4b, in the fully unfolded state [CN(K:O6) = 0], the G8 and T9 bases of the TGT-loop display the aggregated [R_g(8,9) = 3.8 Å] and nonaggregated [R_g(8,9) = 7.0 Å] forms. The aggregated form is more stable than the nonaggregated one. In the folded state [CN(K:O6) = 8], the most distributed conformer is also the base stacking form of G8 and T9. What is striking is that only the aggregated form is directly associated with the incorporation of K^+ to the O6 atoms of the unfolded G-stem. This implies that the base interaction of G8 and T9 in the TGT-loop produces an intermediate state for driving the cation binding in the G-stem folding.

Since the G6 and G10 bases are directly connected to the TGT-loop as neighbors and they partially constitute the upper quadrant of the G-stem (see Figure 1), we investigated if such aggregation of G8 and T9 can influence the packing state of the G6 and G10 bases. Figure 5a represents the 2D free-energy map with R_g(8,9) and R_g(6,10), where R_g(6,10) is the radius of gyration of the G6 and G10 bases. A single-well picture of this map indicates that the aggregation of G8 and T9 in the TGT-loop brings the G6 and G10 bases into close contact as the major population (Figure 5a). The stability of the G-stem is contributed in part from the Hoogsteen base orientation of the coplanar G-tetrad.[34] To investigate such base orientations of G6 and G10 upon the base stacking of G8 and T9, the glycosidic torsions (χ) were computed for both G6 and G10 bases. The χ value can specify two possible base orientations of *anti* and *syn* for nucleic acids. The 2D free energy maps with χ(G6) vs R_g(8,9) and χ(G10) vs R_g(8,9) are given in Figure 5b, c. Both free energy surfaces confirmed that as the G8 and T9 bases come into contact, the base orientations of G6 and G10 approach the native-like ones (*anti*−*syn* form). Therefore, the aggregation of the G8 and T9 bases in the prefolded TGT-loop initiates the G-quadruplex formation.

Role of the TT-Loop in the Folding Process. For the formation of specific tertiary structure of the aptamer/cation complex, it is critical how to form not only the TGT-loop but also two TT-loop regions. The two TT-loops in TBA-15 are known to participate in the binding mode with the heparin binding site of thrombin.[9] In the TBA-15 folding process, however, the role of the TT-loops has not been fully understood. To address this concern, the free-energy map with the rmsd of each TT-loop and the CN value between K^+ and O6 atoms is given in Figure 6. In a similar manner to the TGT-loop, in unfolded states at 288 K, a preliminary form of both TT-loops with rmsd = 3.0 Å exists, which contains a somewhat loosely formed loop turn. As the fully folded state of the G-stem is reached, the TT-loops retain their well-defined native-like character (rmsd = 1.5 Å). Therefore, we can see that the presence of the preformed TT-loops along with the conserved TGT-loop helps the G-stem to fold by significantly reducing the conformational space that the unfolded G-stem can access.

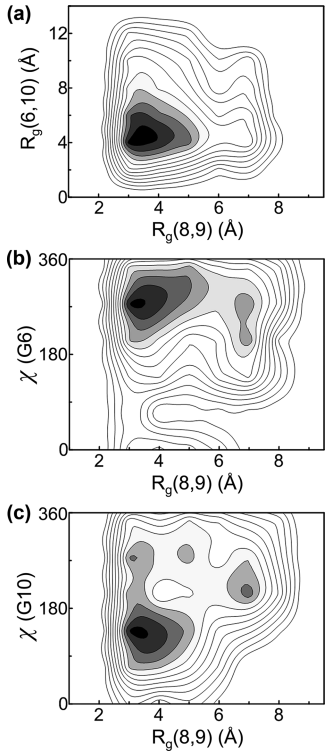

Figure 5. (a)2D free-energy map with respect to the radius of gyration of G8 and T9 bases in TGT-loop R_g(8,9) and the radius of gyration of the G6 and G10 bases R_g(6,10) at 288 K. The 2D free-energy surface with respect to R_g(8,9) and the glycosidic torsion (χ) of G6 (b) and G10 (c) at 288 K. The torsion angle is defined by O4′−C1′−N9−C4 for purine. The χ values of 0 ± 90° and 180 ± 90° are defined as *syn* and *anti* conformations, respectively. In the NMR native structure (PDB entry: 1C34), the χ values of G6 and G10 are 300°(*anti*) and 120°(close to *syn*), respectively. The line interval is about 0.5 kcal/mol in the map.

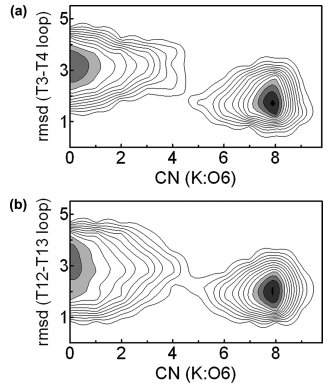

Figure 6. 2D free-energy maps in terms of the CN (K:O6) value and (a) the backbone rmsd of the G2-T3-T4-G5 residues (T3-T4 loop) and (b) the backbone rmsd of the G11-T12-T13-G14 residues (T12-T13 loop) at 288 K. The line interval is about 0.5 kcal/mol in the map.

Cation Capture by the G-Stem. For in-depth analysis on how the cation binds to the G-stem, six individual planes of the two coplanar G-quadruplexes were defined: the upper plane (G1−G6−G10−G15), the lower plane (G2-G5-G11-G14), the front plane (G1−G2−G14−G15), the back plane (G5-G6-G10-G11), the 5′-end side plane (G1−G2−G5−G6), and the

3′-end side plane (G10−G11−G14−G15). Then, the radius of gyration of the four O6 atoms R_g(O6) on each plane was computed to represent an ordering state of each plane during the formation of the G-quadrants. Since R_g(O6) decreases as the native G-quadrants are formed, this coordinate can give direct information on the ordering state of the G-stem residues projected into any given plane described above. Figure 7 shows

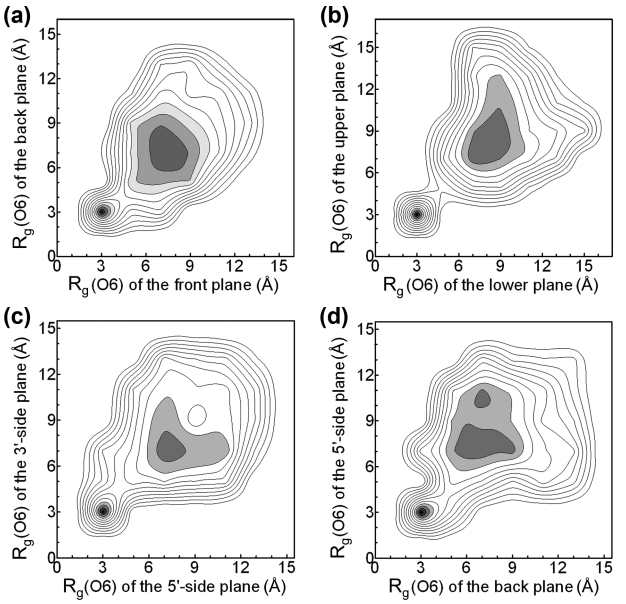

Figure 7. Free-energy maps as a function of the radius of gyrations of the carboxylic oxygen atoms (O6) of (a) the back plane vs the front plane, (b) the lower plane vs the upper plane, (c) 5′-side plane vs 3′-side plane, and (d) the back plane vs 5′-side plane at 288 K. Each face of the chairlike G-stem is defined as the upper plane (G1−G6−G10−G15), the lower plane (G2−G5−G11−G14), the front plane (G1−G2−G14−G15), the back plane (G5−G6−G10−G11), one side plane from 5′-end (G1−G2−G5−G6), and the other side plane from 3′-end (G10−G11−G14−G15). The line interval is about 0.5 kcal/mol in the map.

the free energy surface in terms of any two R_g(O6) values. Any combinations of two R_g(O6) values give a similar free-energy pattern. Furthermore, the ordering states of any two planes are strongly correlated. Therefore, we found that the G-quadruplexes are created by the concurrent complexation of K^+ with all eight O6 atoms in the G-stem.

Dehydration in the Folding Process. One of the interesting phenomena in the TBA-15 folding is that, as the G-quadrants are formed, the water molecules solvating the guanine bases in the G-stem are dehydrated.[11] To provide more quantitative analyses of dehydration status around the O6 atoms during the TBA-15 folding, the free-energy profile as a function of the number of water molecules near the O6 atoms (cutoff =3.5 Å) is given in Figure 8. The result indicates that the dehydration state of the O6 atoms is a well-defined progressive variable governing the overall aptamer folding characteristics. As seen in Figure 8, in the fully unfolded states, the O6 atoms were solvated by 21 water molecules. In the transition state, as a result of the dehydration process, 7−8 water molecules were found near the O6 atoms. In the native state, the water molecules were excluded entirely from the interior region of the G-quadruplexes. Although 2−3 water molecules still existed around the O6 atoms, they were mostly located between the TGT-loop and the upper quadruplex plane.

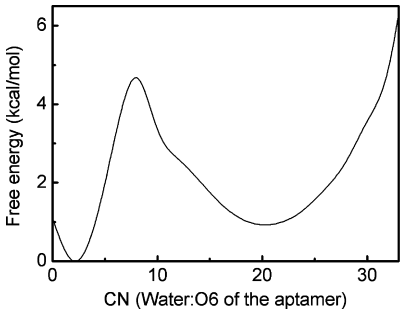

Figure 8. Free-energy profile as a function of the number of water molecules near the eight O6 atoms in the G-stem at 288 K. A distance cutoff of 3.5 Å was used to count this number.

Folding Pathway of TBA-15. The overall folding pictures based on our analysis of the free-energy maps in various combinations of the reaction coordinates are depicted in Figure 9. The representatives were obtained by cluster analysis based

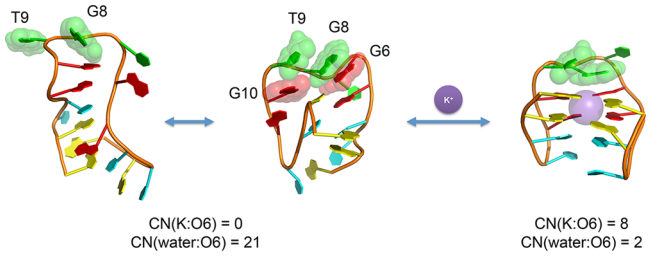

Figure 9. Folding pathway of the TBA-15/K^+ complex. In the G-stem, the front plane (G1−G2−G14−G15) and the back plane (G5−G6−G10−G11) residues are colored yellow and red, respectively. The TT-loop bases are presented in cyan and the TGT-loop bases are depicted in green. To show the base stacking interaction in the TGT-loop, the base pairs of G8/T9 and G6/G10 are drawn with a transparent sphere. Each structure is extracted by cluster analysis.

on rmsd.[35] As indicated in Figure 9, it is evident that the base stacking of the G8 and T9 in the TGT-loop facilitates the G-stem folding by creating more favorable environments for the cation binding. In the unfolded G-stem without the G8/T9 stacking, a series of non-native base-stacking interactions in the G-stem led to unrealistic arrangements for the incorporation of the K^+ ion. However, when the G8 and T9 bases of the TGT-loop come into close contact, the native-like *anti−syn* base ordering of the G6 and G10 bases occurs in the G-stem, although the correct hydrogen bonds between the neighbor guanines are not formed. This induced base ordering of G6 and G10 also affects the base orientations of the neighboring G5 and G11 residues, in such a way as to create additional base stacking interactions of G5:G6 and G10:G11. Therefore, as a result of the base stacking of the G8 and T9, at least the base orientation of the back plane (G5−G6−G10−G11) is approximately restored to their native-like one. Also, the other G-stem bases are reoriented to more plausible positions for accommodating the metal cation (see Figure 9).

CONCLUSION

TBA-15 is a single-stranded DNA segment with a wide range of potential applications. This aptamer can fold into a very stable intramolecular G-quadruplex structure in the presence of specific metal cations. To investigate the detailed folding characteristics of this molecule, we performed all-atom REMD

dx.doi.org/10.1021/ct300714u | J. Chem. Theory Comput. 2012, 8, 4845−4851

simulation on the TBA-15/K^+ complex and obtained the free-energy maps with respect to various combinations of reaction coordinates. The interpretations of these free-energy landscapes enable us to shed light on the folding of this complex. One notable feature in the TBA-15 folding is the presence of preformed TGT- and TT-loop geometries prior to the G-stem folding. Thus, the only structural difference between the folded and unfolded states is whether the native G-quadrants are formed. In a fully unfolded state, the TGT-loop structure displays either the stacking or the nonstacking form of the G8-T9 base pair. This base stacking in the prefold TGT-loop serves two purposes. This stacking improves the TGT-loop stability while reducing dynamic fluctuations around the G8 residue. Furthermore, it accompanies preliminary native-like base orientations of the G6 and G10 pair to establish early formation of the upper tetrad. Most interestingly, between the stacking and nonstacking forms of G8 and T9, only the stacking form is apparently related to the cation binding with the G-stem. Upon K^+ binding to the residues of the unfolded G-stem, the native G-quadruplexes are formed in a concerted way at the expense of substantial dehydration. In fact, the K^+ ion can enter the binding pocket of the unfolded G-stem from all directions.

One major concern in this study is the validity of the empirical force field we have employed. According to a recent work,[20] the presently available force fields including several versions of the AMBER and CHARMM force fields are not accurate enough to describe G-DNA loops. Among them, param99bsc0 produced reasonable results conforming to the experimental data despite some discrepancies in the loop prediction. In general, a single stranded DNA hairpin loop topologies posed a major hurdle for molecular mechanical force fields. Thus, more refined force field needs to be developed for better description of loop structures for nucleic acids. For the potassium ion parameter, as fully stated by Joung et al.,[36] the main problem of the standard amber force field for K^+ is the salt crystallization with Cl^- ion as an artifact. This article mentioned above showed that the repulsive interaction in the standard amber force field for K^+ was overestimated for short-range. Properly optimized or reduced van der Waals radius would overcome the lack of balance between ion−ion interactions. Originally, the amber cation parameters were obtained by closely reproducing experimental solvation free energy data.[27] Therefore, reducing the radius can also adversely affect the accuracy of ion−water interactions. As discussed by Reshetnikov et al.,[23] the aforementioned salt crystallization problems in the standard AMBER potassium parameter may not be important for describing the mechanism of the cation binding to TBA-15. At this point, it remains to be seen that use of modified ion parameters can further improve the free energy landscape of the G-DNA/K^+ complex in explicit water environments.

AUTHOR INFORMATION

Corresponding Author

*E-mail: ypak@pusan.ac.kr.

Notes

The authors declare no competing financial interest.

ACKNOWLEDGMENTS

Y.P. thanks National Research Foundation of Korea (2010-0015929) for the financial support.

REFERENCES

(1) Neidle, S. The structures of quadruplex nucleic acids and their drug complexes. *Curr. Opin. Struct. Biol.* **2009**, *19*, 239−250.

(2) Jiang, Y. L.; Liu, Z. P. Metallo-organic G-quadruplex ligands in anticancer drug design. *Mini-Rev. Med. Chem.* **2010**, *10*, 726−736.

(3) Cummaro, A.; Fotticchia, I.; Franceschin, M.; Giancola, C.; Petraccone, L. Binding properties of human telomeric quadruplex multimers: A new route for drug design. *Biochimie* **2011**, *93*, 1392−1400.

(4) Ralph, S. F. Quadruplex DNA: A promising drug target for the medicinal inorganic chemist. *Curr. Top. Med. Chem.* **2011**, *11*, 572−590.

(5) Xing, H.; Wong, N. Y.; Xiang, Y.; Lu, Y. DNA aptamer functionalized nanomaterials for intracellular analysis, cancer cell imaging, and drug delivery. *Curr. Opin. Chem. Biol.* **2012**, *16*, 429−435.

(6) Schultze, P.; Macaya, R. F.; Feigon, J. Three-dimensional solution structure of the thrombin-binding DNA aptamer d(GGTTGGTGTGGTTGG). *J. Mol. Biol.* **1994**, *235*, 1532−1547.

(7) Marathias, V. M.; Bolton, P. H. Structures of the potassium-saturated, 2:1, and intermediate, 1:1, forms of a quadruplex DNA. *Nucleic Acids Res.* **2000**, *28*, 1969−1977.

(8) Padmanabhan, K.; Padmanabhan, K. P.; Ferrara, J. D.; Sadler, J. E.; Tulinsky, A. The structure of α-thrombin inhibited by a 15-mer single-stranded DNA aptamer. *J. Biol. Chem.* **1993**, *268*, 17651−17654.

(9) Nagatoishi, Satoru; Isono, Noburu; Tsumoto, Kouhei; Sugimoto, N. Loop residues of thrombin-binding DNA aptamer impact G-quadruplex stability and thrombin binding. *Biochimie* **2011**, *93*, 1231−1238.

(10) Mao, X. A.; Gmeiner, W. H. NMR study of the folding-unfolding mechanism for the thrombin-binding DNA aptamer d(GGTTGGTGTGGTTGG). *Biophys. Chem.* **2005**, *113*, 155−160.

(11) Kankia, B. I.; Marky, L. A. Folding of the Thrombin aptamer into a G-Quadruplex with Sr^{2+}: Stability, Heat, and Hydration. *J. Am. Chem. Soc.* **2001**, *123*, 10799−10804.

(12) Silva, M. W. Geometric formalism for DNA quadruplex folding. *Chem.—Eur. J.* **2007**, *13*, 9738−9745.

(13) Smirnov, I.; Shafer, R. H. Effect of loop sequence and size on DNA aptamer stability. *Biochemistry* **2000**, *39*, 1462−1468.

(14) Hardin, C. C.; Perry, A. G.; White, K. Thermodynamic and kinetic characterization of the dissociation and assembly of quadruplex nucleic acids. *Biopolymers* **2001**, *56*, 147−194.

(15) Olsen, C. M.; Gmeiner, W. H.; Marky, L. A. Unfolding of G-quadruplexes: Energetic and ion and water contributions of G-quartet stacking. *J. Phys. Chem. B* **2006**, *110*, 6962−6969.

(16) Miyoshi, D.; Karimata, H.; Sugimoto, N. Hydration regulates thermodynamics of G-quadruplex formation under molecular crowding conditions. *J. Am. Chem. Soc.* **2006**, *128*, 7957−7963.

(17) Pagano, B.; Mattia, C. A.; Virno, A.; Randazzo, A.; Mayol, L.; Giancola, C. Thermodynamic analysis of quadruplex DNA-drug interaction. *Nucleosides Nucleotides Nucleic Acids* **2007**, *26*, 761−765.

(18) Shim, J. W.; Tan, Q.; Gu, L. Q. Single-molecule detection of folding and unfolding of the G-quadruplex aptamer in a nanopore nanocavity. *Nucleic Acids Res.* **2009**, *37*, 972−982.

(19) van der Spoel, D.; Seibert, M. M. Protein folding kinetics and thermodynamics from atomistic simulations. *Phys. Rev. Lett.* **2006**, *96*, 238102.

(20) Fadrna, E.; Spackova, N.; Sarzynska, J.; Koca, J.; Orozco, M.; Cheatham, T. E.; Kulinski, T.; Sponer, J. Single Stranded loops of quadruplex DNA as key benchmark for testing nucleic acids force fields. *J. Chem. Theory Comput.* **2009**, *5*, 2514−2530.

(21) Reshetnikov, R.; Golovin, A.; Spiridonova, V.; Kopylov, A.; Sponer, J. Structural dynamics of thrombin-binding DNA Aptamer d(GGTTGGTGTGGTTGG) quadruplex DNA studied by large-scale explicit solvent simulations. *J. Chem. Theory Comput.* **2010**, *6*, 3003−3014.

(22) Reshetnikov, R. V.; Golovin, A. V.; Kopylov, A. M. Comparison of models of thrombin-binding 15-mer DNA aptamer by molecular dynamics simulation. *Biochemistry (Moscow)* **2010**, *75*, 1017−1024.

(23) Reshetnikov, R. V.; Sponer, J.; Rassokhina, O. I.; Kopylov, A. M.; Tsvetkov, P. O.; Makarov, A. A.; Golovin, A. V. Cation binding to 15-TBA quadruplex DNA is a multiple-pathway cation-dependent process. *Nucleic Acids Res.* **2011**, *39*, 9789−9802.
(24) Yang, C.; Jang, S.; Pak, Y. Multiple stepwise pattern for potential of mean force in unfolding the thrombin binding aptamer in complex with Sr^{2+}. *J. Chem. Phys.* **2011**, *135*, 225104.
(25) Jorgensen, W. L.; Chandrasekhar, J.; Madura, J. D.; Impey, R. W.; Klein, M. L. Comparison of simple potential functions for simulating liquid water. *J. Chem. Phys.* **1983**, *79*, 926−935.
(26) Perez, A.; Marchan, I.; Svozil, D.; Sponer, J.; Cheatham, T. E., III; Laughton, C. A.; Orozco, M. Refinement of the AMBER force field for nucleic acids: Improving the description of α/γ conformers. *Biophys. J.* **2007**, *92*, 3817−3829.
(27) Ross, W. S.; Hardin, C. C. Ion-induced stabilization of the G-DNA quadruplex: Free energy perturbation studies. *J. Am. Chem. Soc.* **1994**, *116*, 6070−6080.
(28) Sugita, Y.; Okamoto, Y. Replica-exchange molecular dynamics method for protin folding. *Chem. Phys. Lett.* **1999**, *314*, 141−151.
(29) Bussi, G.; Donadio, D.; Parrinello, M. Canonical sampling through velocity rescaling. *J. Chem. Phys.* **2007**, *126*.
(30) Hess, B. P-LINCS: A parallel linear constraint solver for molecular simulation. *J. Chem. Theory Comput.* **2008**, *4*, 116−122.
(31) Darden, T.; York, D.; Pedersen, L. G. Particle mesh Ewald: An $N\log(N)$ method for Ewald sums in large systems. *J. Chem. Phys.* **1993**, *98*, 10089−10092.
(32) Essmann, U.; Perera, L.; Berkowitz, M. L.; Darden, T.; Lee, H.; Pedersen, L. G. A smooth particle mesh Ewald potential. *J. Chem. Phys.* **1995**, *103*, 8577−5892.
(33) Hess, B.; Kutzner, C.; van der Spoel, D.; Lindahl, E. GROMACS 4: Algorithms for highly efficient, load-balanced, and scalable molecular simulation. *J. Chem. Theory Comput.* **2008**, *4*, 435−447.
(34) Cang, X.; Sponer, J.; Cheatham, T. E., III Explaining the varied glycosidic conformational, G-tract length, and sequence preferences for anti-parallel G-quadruplexes. *Nucleic Acids Res.* **2011**, *39*, 4499−4512.
(35) Daura, X.; Gademann, K.; Jaun, B.; Seebach, D.; Gunsteren, W. F. v.; Mark, A. E. Peptide folding: When simulation meets experiment. *Angew. Chem., Int. Ed.* **1999**, *38*, 236−240.
(36) Joung, I. S.; Cheatham, T. E., III Determination of alkali and halide monovalent ion parameters for use in explicitly solvated biomolecular simulations. *J. Phys. Chem. B* **2008**, *112*, 9020−9041.